


RESEARCH ARTICLE | OCTOBER 10 2012

Pressure dependence of the Verwey transition in magnetite: An infrared spectroscopic point of view

J. Ebad-Allah; L. Baldassarre; M. Sing; R. Claessen; V. A. M. Brabers; C. A. Kuntscher

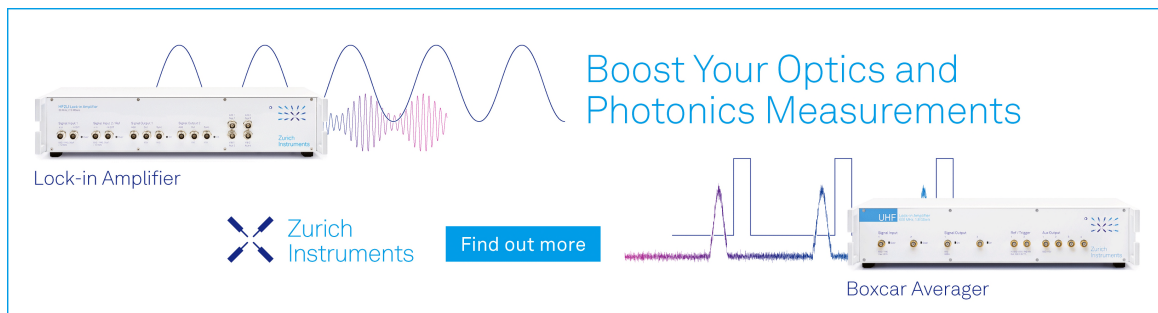
 Check for updates

J. Appl. Phys. 112, 073524 (2012)


<https://doi.org/10.1063/1.4758303>



Boost Your Optics and Photonics Measurements



Lock-in Amplifier

 Zurich Instruments

[Find out more](#)

Boxcar Averager

Pressure dependence of the Verwey transition in magnetite: An infrared spectroscopic point of view

J. Ebad-Allah,¹ L. Baldassarre,¹ M. Sing,² R. Claessen,² V. A. M. Brabers,² and C. A. Kuntscher^{a)}

¹*Experimentalphysik 2, Universität Augsburg, D-86195 Augsburg, Germany*

²*Physikalisches Institut, Universität Würzburg, D-97074 Würzburg, Germany*

(Received 13 July 2012; accepted 12 September 2012; published online 10 October 2012)

We investigated the electronic and vibrational properties of magnetite at temperatures from 300 K down to 10 K and for pressures up to 10 GPa by far-infrared reflectivity measurements. The Verwey transition is manifested by a drastic decrease of the overall reflectance and the splitting of the phonon modes as well as the activation of additional phonon modes. In the whole studied pressure range, the down-shift of the overall reflectance spectrum saturates and the maximum number of phonon modes is reached at a critical temperature, which sets a lower bound for the Verwey transition temperature T_v . Based on these optical results, a pressure-temperature phase diagram for magnetite is proposed. © 2012 American Institute of Physics.

[<http://dx.doi.org/10.1063/1.4758303>]

I. INTRODUCTION

Numerous experimental studies have been carried out on the natural mineral magnetite (Fe_3O_4) to understand its puzzling electronic and magnetic properties. It is the oldest known magnetic material and the prototype material for the Verwey transition, which leads to charge ordering.¹ Fe_3O_4 has an inverse cubic spinel structure at ambient conditions and is in a mixed-valence state described as $[\text{Fe}^{3+}]_A[\text{Fe}^{2+} + \text{Fe}^{3+}]_B\text{O}_4$, where A and B denote the tetrahedral and octahedral sites, respectively, in the spinel structure AB_2O_4 , with space group $\text{Fd}\bar{3}m$.² At ambient conditions, magnetite can be classified as a bad metal due to the presence of a small Drude contribution.^{3–5} With decreasing temperature, magnetite undergoes a metal-to-insulator transition at the so-called Verwey transition temperature $T_v \approx 120$ K, concurrent with a lowering of the crystal structure symmetry from cubic to monoclinic.^{6–9} Various experimental investigations led to contradictory scenarios for the rearrangement of charges on the Fe sites and the resulting charge ordering below T_v .^{10–15} In contrast, consistent results have been obtained by various groups^{3–5} regarding the changes in the optical properties when cooling below T_v : According to infrared reflectivity measurements as a function of temperature, a clear opening of a charge gap (≈ 0.14 eV) and the appearance of numerous infrared modes due to the crystal symmetry lowering were observed.

Besides the charge ordering pattern below T_v , a matter of controversy is furthermore the behavior of T_v as a function of pressure. Resistivity measurements^{16,17} showed a sharp drop of T_v at the critical pressure $P_c = 7 - 8$ GPa to zero and a metallization above P_c . This finding was confirmed later on by ac magnetic susceptibility together with resistivity measurements.¹⁸ In Ref. 18, furthermore the existence of a quantum

critical point in the pressure-temperature phase diagram of magnetite was claimed.¹⁸ In contradiction to these results, several groups found a linear decrease of T_v with increasing pressure based on resistivity measurements, with a linear pressure coefficient of either -2.8 K/GPa^{19–21} or -5 K/GPa.^{22,23} A recent Raman study confirmed the linear decrease of T_v with -5 K/GPa.²⁴ The absence or presence of a quantum critical point could be related to the level of hydrostaticity in the pressure cell, which may vary for the different types of experiments. Also, the measurement technique might play a role.

The above-mentioned controversy regarding $T_v(P)$ motivated us to study the Verwey transition in magnetite as a function of pressure by far-infrared reflectivity measurements, which comprise both electronic and vibrational properties. The goal of our investigation is not primarily the precise determination of the pressure dependence of the Verwey transition temperature like in other studies, but to characterize the phases of magnetite close to the Verwey transition from an infrared spectroscopic point of view: The overall level of the reflectance spectrum and the phonon mode activation and splitting are considered for various temperatures and pressures. Based on these two criteria, we propose a pressure-temperature phase diagram. We also relate our results to those of earlier works.

II. METHODS

The single crystals of magnetite used in this work were grown from polycrystalline Fe_3O_4 bars by using a floating-zone technique with radiation heating.²⁵ The polycrystalline bars were prepared from $\alpha\text{-Fe}_2\text{O}_3$ by the usual ceramic procedures as pressing and sintering in an adapted oxygen atmosphere. The quality of the crystals was checked by electrical transport measurements, showing a sharp increase of the resistivity by a factor of about 100 at the critical temperature $T_v \approx 122$ K, which is characteristic for the Verwey transition.²⁶ The low-temperature reflectance measurements under pressure were conducted in the frequency range from

^{a)}Present address: Department of Physics, Eindhoven University of Technology, 5600 MB Eindhoven, The Netherlands. Electronic mail: christine.kuntscher@physik.uni-augsburg.de.

200 to 700 cm^{-1} with a frequency resolution 1 cm^{-1} partly at the infrared beamline of the synchrotron radiation source ANKA and partly in the lab at Augsburg university. A clamp diamond anvil cell (Diacell cryoDAC-Mega) equipped with type IIA diamonds, which are suitable for infrared measurements, was used for the generation of pressures up to 10 GPa. Finely, ground CsI powder was used as quasi-hydrostatic pressure transmitting medium, in order to ensure a well-defined sample-diamond interface throughout the experiment. The pressure in the diamond anvil cell (DAC) was determined *in situ* in the cryostat by the ruby luminescence method.²⁷ The width of the phonon modes in the measured high-pressure reflectance spectra is comparable to that reported earlier on samples at ambient conditions,³ evidencing the quasi-hydrostatic conditions in the DAC.

The reflectance measurements at low temperature and high pressure were carried out using a home-built infrared microscope coupled to the FTIR spectrometer and maintained at the same vacuum conditions, in order to avoid absorption lines of H_2O and CO_2 molecules. The infrared radiation was focused on the sample by all-reflecting Schwarzschild objectives with a large working distance of about 55 mm and 14 \times magnification. The DAC was mounted in a continuous-flow helium cryostat (Cryo Vac KONTI cryostat). More details about the geometry of the reflectivity measurements can be found in our earlier publications.^{28,29} As reference, we used the intensity reflected from the CuBe gasket inside the DAC. All reflectance spectra shown in this paper refer to the absolute reflectance at the sample-diamond interface, denoted as R_{s-d} . Furthermore, corrections regarding the decaying intensity of the synchrotron radiation with time have been taken into account.

III. RESULTS AND DISCUSSION

The far-infrared reflectance spectrum of magnetite was measured for several pressures between 0 and 10 GPa as a function of temperature. As an example, we show in Fig. 1(a), the reflectance spectrum at ≈ 2.5 GPa for various temperatures. At room temperature, two oxygen phonon modes are observed with frequencies close to 355 cm^{-1} and 565 cm^{-1} at low pressure, consistent with earlier reports.^{3-5,26,30} While cooling down from room temperature to 150 K, which is well above T_v ,¹⁷⁻²⁴ the overall reflectance spectrum gradually decreases [see Fig. 1(a)], consistent with a “bad metal” behavior also found in temperature-dependent dc resistivity data.²⁶ Below ≈ 150 K, the overall reflectance decreases drastically with a saturation below ≈ 102 K. Furthermore, below 150 K, the reflectance spectrum becomes more complex because of the phonon mode splitting and the activation of additional low-frequency phonon modes. By comparing the temperature dependence of the reflectance spectra for two pressures (2.5 and 7.8 GPa), as depicted in Figs. 1(a) and 1(b), it is obvious that this overall evolution of the reflectance spectrum with decreasing temperature is not strongly dependent on the applied pressure. Furthermore, at a fixed temperature, the overall reflectance spectrum is enhanced with increasing pressure, which is consistent with the pressure-induced increase of the conductivity according to dc transport measurements.¹⁷

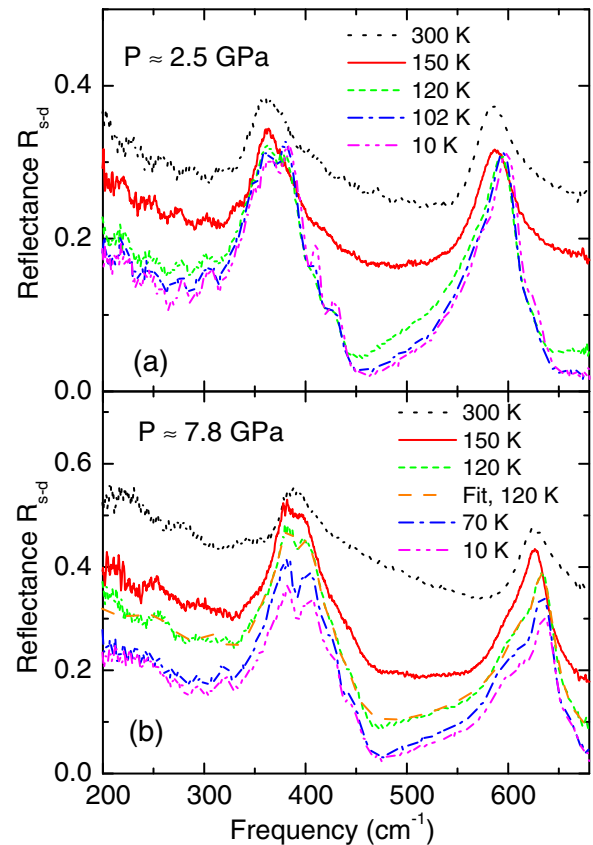


FIG. 1. Reflectance spectrum of magnetite for various temperatures at around (a) 2.5 GPa and (b) 7.8 GPa. In (b), additionally the fitting curve based on the Drude-Lorentz model for the reflectance spectrum at 120 K is shown.

For a quantitative characterization of the pressure- and temperature-induced changes in the optical response, the reflectance spectra were fitted according to the Fresnel equation for normal-incidence reflectivity taking into account the diamond-sample interface

$$R_{s-d} = \left| \frac{n_{\text{dia}} - \sqrt{\epsilon_s}}{n_{\text{dia}} + \sqrt{\epsilon_s}} \right|^2; \quad \epsilon_s = \epsilon_\infty + \frac{i\sigma}{\epsilon_0\omega}, \quad (1)$$

where n_{dia} is the refractive index of diamond and assumed to be independent of pressure and temperature, and ϵ_s is the complex dielectric function of the sample. From the function $\epsilon_s(\omega)$, the real part of the optical conductivity, $\sigma_1(\omega)$, can be calculated according to Eq. (1), where ϵ_∞ is the background dielectric constant (here $\epsilon_\infty \approx 1$). $\epsilon_s(\omega)$ was assumed to follow the Drude-Lorentz model.³¹ An example for the fitting is depicted in Fig. 1(a) for $T = 120$ K at $P = 7.8$ GPa: To obtain a good fit of the reflectance spectrum, we had to include a Drude term and several Lorentz oscillators describing the phonon modes, while the high-frequency extrapolation was modeled according to ambient-temperature data.²⁶ It is important to note here that the extrapolations are not significant for our conclusions (see below) on the pressure-temperature phase diagram of magnetite. The various excitations (Drude term, phonon modes) at $T = 120$ K and 7.8 GPa are illustrated in Fig. 2(a) together with the real part of the optical conductivity within the measured frequency range. At the

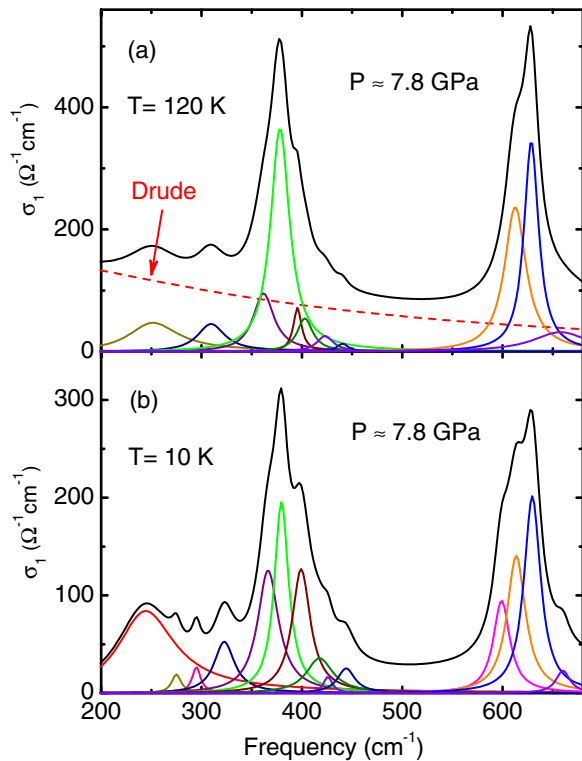


FIG. 2. Real part of the optical conductivity of magnetite at 7.8 GPa and (a) 120 K and (b) 10 K, obtained from the fitting of the reflectance spectra with the Drude-Lorentz model. The contributions (Lorentz oscillators; Drude term at 120 K) based on the fitting are also shown.

lowest studied temperature (10 K), the optical conductivity can be described as a sum of Lorentz oscillators reflecting the rich phonon spectrum below T_V [see Fig. 2(b)].

As a criterium for entering the charge-ordered state one can take the saturation of the down-shift of the reflectance spectrum (see Fig. 1) and the absence of a Drude term. Concomitant with the overall lowering of the reflectance spectrum occurs the splitting of the phonon modes and the activation of additional modes. The mode splitting and activation are manifestations of symmetry lowering of the crystal structure (from cubic to monoclinic) at the Verwey transition.³⁻⁵ Therefore, reaching the maximum number of phonon modes serves as an additional criterium for entering the charge-ordered phase. The temperature-dependent phonon spectrum was characterized based on the Drude-Lorentz fitting, and the extracted mode frequencies are shown in Fig. 3 at 2.5 and 7.8 GPa. Interestingly, the splitting and activation of phonon modes already start at around 150 K, i.e., well above T_V , in agreement with earlier infrared studies.^{5,32} The temperature at which a saturation regarding the down-shift of the reflectance spectrum and the number of phonon modes is reached sets a lower bound for T_V .

Based on two criteria—the down-shift of the reflectance spectrum and the phonon mode splitting/activation—we can mark the “bad metal” and insulating phases in the pressure-temperature phase diagram of magnetite, as shown in Fig. 4. The most important result is that we do not observe a suppression of the insulating state even at the highest pressure applied (10 GPa), in agreement with some earlier studies.¹⁹⁻²⁴ We do not observe the metallization of magnetite above

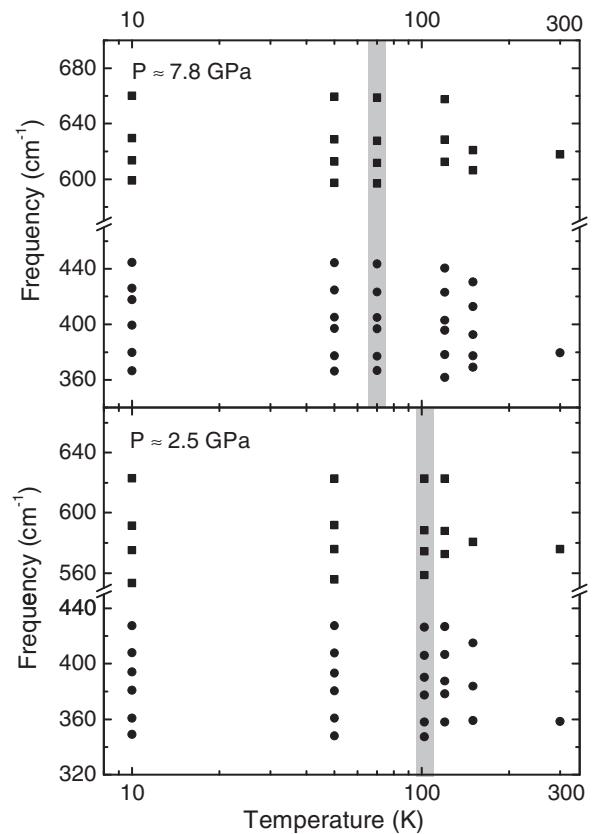


FIG. 3. Splitting of the two phonon modes and activation of phonon modes with decreasing temperature at 2.5 and 7.8 GPa. At a critical temperature (marked by a gray bar), the maximum number of phonon modes is reached.

≈ 8 GPa and the occurrence of a quantum critical point, as claimed in other works.^{16-18,33} Whether or not this is due to the quasi-hydrostatic conditions in the DAC remains an open question, as no systematic study on the pressure dependence

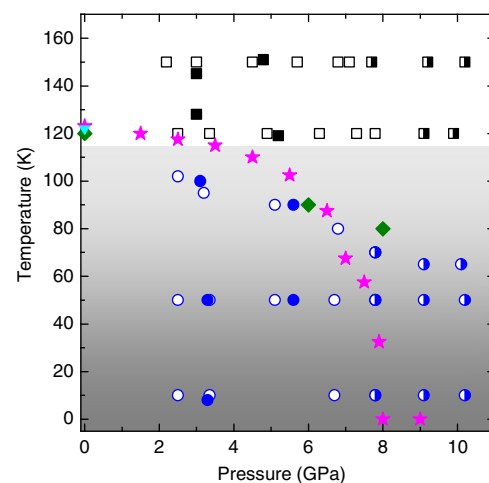


FIG. 4. Pressure-temperature phase diagram of magnetite for temperatures below 160 K and pressures up to ≈ 10 GPa. The squares correspond to the “bad metal” state and the circles to the insulating state. The results from three data sets are distinguished by empty, filled, and half-filled symbols. The gray region indicates the charge-ordered, insulating phase as observed by our optical data. The Verwey transition temperature based on earlier dc transport measurements at ambient pressure is marked by the filled down triangle.²⁶ The results for the Verwey transition temperature T_V of Ref. 17 are marked by filled stars and those of Ref. 24 by filled diamonds.

of the Verwey transition temperature in the same sample for various pressure transmitting media exists.

IV. CONCLUSION

In conclusion, based on the temperature- and pressure-dependent optical response of magnetite, we find the typical signatures of the Verwey transition, namely (i) the overall lowering of the reflectance related to the entering of the charge-ordered state, and (ii) the splitting and activation of phonon modes due to the lowering of the crystal symmetry. The downshift of the reflectance spectrum and the splitting/activation of phonon modes are completed at a critical temperature, which sets a lower bound for T_V . Based on these results, we propose a phase diagram for magnetite showing the “bad metal” and the insulating phases. The metallization of magnetite above ≈ 8 GPa and the occurrence of a quantum critical point is not observed in our data.

ACKNOWLEDGMENTS

We acknowledge the ANKA Angströmquelle Karlsruhe for the provision of beamtime and thank B. Gasharova, Y.-L. Mathis, D. Moss, and M. Süpfle for assistance using the beamline ANKA-IR. We thank K. Syassen for providing valuable information about the construction of the home-made infrared microscope. This work was financially supported by the German Science Foundation (DFG) through SFB 484.

¹E. J. W. Verwey, *Nature (London)* **144**, 327 (1939).

²S. Sasaki, *Acta Crystallogr. B* **53**, 762 (1997).

³L. Degiorgi, I. Blatter-Mörke, and P. Wachter, *Phys. Rev. B* **35**, 5421 (1987).

⁴S. K. Park, T. Ishikawa, and Y. Tokura, *Phys. Rev. B* **58**, 3717 (1998).

⁵L. V. Gasparov, D. B. Tanner, D. B. Romero, H. Berger, G. Margaritondo, and L. Forró, *Phys. Rev. B* **62**, 7939 (2000).

⁶M. Iizumi, *Acta Crystallogr., Sect. B: Struct. Crystallogr. Cryst. Chem.* **38**, 2121 (1982).

⁷J. P. Wright, J. P. Attfield, and P. G. Radaelli, *Phys. Rev. Lett.* **87**, 266401 (2001).

⁸J. P. Wright, J. P. Attfield, and P. G. Radaelli, *Phys. Rev. B* **66**, 214422 (2002).

⁹M. S. Senn, J. P. Wright, and J. P. Attfield, *Nature* **481**, 173 (2012).

¹⁰E. Nazarenko, J. E. Lorenze, Y. L. Hodeau, D. Mannix, and C. Marin, *Phys. Rev. Lett.* **97**, 056403 (2006).

¹¹H. Kobayashi, *Phys. Rev. B* **73**, 104110 (2006).

¹²M. P. Pasternak, W. M. Xu, G. Kh. Rozenberg, R. D. Taylor, and R. Jeanloz, *Magn. Magn. Mater.* **265**, L107 (2003).

¹³G. Kh. Rozenberg, Y. Amiel, W. M. Xu, M. P. Pasternak, R. Jeanloz, M. Hanfland, and R. D. Taylor, *Phys. Rev. B* **75**, 020102 (2007).

¹⁴S. V. Ovsyannikov, V. V. Shchennikov, S. Todo, and Y. Uwatoko, *J. Phys.: Condens. Matter* **20**, 172201 (2008).

¹⁵F. Baudelet, S. Pascarelli, O. Mathon, J.-P. Itie, A. Polian, and J.-C. Chervin, *Phys. Rev. B* **82**, 140412(R) (2010).

¹⁶S. Todo, N. Takeshita, T. Kanehara, T. Mori, and N. Môri, *J. Appl. Phys.* **89**, 7347 (2001).

¹⁷N. Môri, S. Todo, N. Takeshita, T. Mori, and Y. Akishige, *Physica B* **312–313**, 686 (2002).

¹⁸J. Spalek, A. Kozłowski, Z. Tarnawski, Z. Kakol, Y. Fukami, F. Ono, R. Zach, L. J. Spalek, and J. M. Honig, *Phys. Rev. B* **78**, 100401(R) (2008).

¹⁹Y. Kakudate, N. Môri, and Y. Kino, *J. Magn. Magn. Mater.* **12**, 22 (1979).

²⁰S. Tamura, *J. Phys. Soc. Jpn.* **59**, 4462 (1990).

²¹G. K. Rozenberg, G. R. Hearne, M. P. Pasternak, P. A. Metcalf, and J. M. Honig, *Phys. Rev. B* **53**, 6482 (1996).

²²G. A. Samara, *Phys. Rev. Lett.* **21**, 795 (1968).

²³S. K. Ramasesha, M. Mohan, A. K. Singh, J. M. Honig, and C. N. R. Rao, *Phys. Rev. B* **50**, 13789 (1994).

²⁴L. V. Gasparov, D. Arenas, K.-Y. Choi, G. Günterth, H. Berger, L. Forro, G. Margaritondo, V. V. Struzhkin, and R. Hemley, *J. Appl. Phys.* **97**, 10A922 (2005).

²⁵V. A. M. Brabers, *J. Cryst. Growth* **8**, 26 (1971).

²⁶J. Ebad-Allah, L. Baldassarre, M. Sing, R. Claessen, V. A. M. Brabers, and C. A. Kuntscher, e-print arXiv:1202.4431.

²⁷H. K. Mao, J. Xu, and P. M. Bell, *J. Geophys. Res.* **91**, 4673, doi:10.1029/JB091iB05p04673 (1986).

²⁸A. Pashkin, M. Dressel, and C. A. Kuntscher, *Phys. Rev. B* **74**, 165118 (2006).

²⁹C. A. Kuntscher, S. Frank, A. Pashkin, M. Hoinkis, M. Klemm, M. Sing, S. Horn, and R. Claessen, *Phys. Rev. B* **74**, 184402 (2006).

³⁰J. Ebad-Allah, L. Baldassarre, M. Sing, R. Claessen, V. A. M. Brabers, and C. A. Kuntscher, *High Press. Res.* **29**, 500 (2009).

³¹F. Wooten, *Optical Properties of Solids* (Academic, New York, 1972).

³²A. Pimenov, S. Tachos, T. Rudolf, A. Loidl, D. Schrupp, M. Sing, R. Claessen, and V. A. M. Brabers, *Phys. Rev. B* **72**, 035131 (2005).

³³G. Kh. Rozenberg, M. P. Pasternak, W. M. Xu, Y. Amiel, M. Hanfland, R. D. Taylor, and R. Jeanloz, *Phys. Rev. Lett.* **96**, 045705 (2006).